DEUTSCHES ELEKTRONEN-SYNCHROTRON
INSTITUT FÜR HOCHENERGIEPHYSIK
DESY 94-049
BAIKAL 93-15
March 1994

The Lake Baikal Telescope NT-36 – A First Deep Underwater Multistring Array

presented by

R. Wischnewski

for the BAIKAL Collaboration

ISSN 0418-9833

PLATANENALLEE 6 - 15738 ZEUTHEN

To be sure that your preprints are promptly included in the
HIGH ENERGY PHYSICS INDEX,
send them to (if possible by air mail):

DESY **Bibliothek** **Notkestraße 85** **22603 Hamburg** **Germany**	**DESY-IfH** **Bibliothek** **Platanenallee 6** **15738 Zeuthen** **Germany**

DESY 94-049 ISSN 0418-9833
BAIKAL 93-15
March 1994

The Lake Baikal Telescope NT-36 – A First Deep Underwater Multistring Array

I.A.Belolaptikov[8], L.B.Bezrukov[1], B.A.Borisovets[1], N.M.Budnev[2], A.G.Chensky[2], Zh.A.M.Djilkibaev[1], V.I.Dobrynin[2], G.V.Domogatsky[1], L.A.Donskych[1], A.A.Doroshenko[1], S.V.Fialkovsky[5], O.A.Gress[2], A.V.Golikov[3], R.Heller[9], H.Heukenkamp[9], V.B.Kabikov[3], A.M.Klabukov[1], A.I.Klimov[7], S.I.Klimushin[1], T.A.Konopleva[2], A.P.Koshechkin[2], J.Krabi[9], V.F.Kulepov[5], L.A.Kuzmichov[3], O.J.Lanin[1], B.K.Lubsandorzhiev[1], M.B.Milenin[5], T.Mikolajski[9], R.R.Mirgazov[2], S.A.Nikiforov[2], N.V.Ogievietzky[1], E.A.Osipova[3], A.H.Padusenko[4], A.I.Panfilov[1], Yu.V.Parfenov[2], A.A.Pavlov[2], D.P.Petuchov[1], K.A.Pocheikin[2], P.G.Pochil[1], O.P.Pokalev[2], M.I.Rosanov[6], A.V.Rzhetshizki[2], V.Yu.Rubzov[2], S.I.Sinegovsky[2], I.A.Sokalsky[1], Ch.Spiering[9], O.Streicher[9], V.A.Tarashansky[2], T.Thon[9], I.I.Trofimenko[1], R.Wischnewski[9], V.L.Zurbanov[2]

presented by R. WISCHNEWSKI

[1] Institute for Nuclear Research, Russian Acad. of Science (Moscow, Russia)
[2] Irkutsk State University (Irkutsk, Russia)
[3] Moscow State University (Moscow, Russia)
[4] Tomsk Polytechnical Institute (Tomsk, Russia)
[5] Polytechnical Institute (Nizhni Novgorod, Russia)
[6] Marine Technical University (St.Petersburg, Russia)
[7] Kurchatov Institute of Atomic Energy (Moscow, Russia)
[8] Joint Institute for Nuclear Research (Dubna, Russia)
[9] DESY Institute for High Energy Physics (Zeuthen, Germany)

Abstract

Since April 13th, 1993 the underwater Cherenkov telescope NT-36, consisting of 36 photomultipliers attached to 3 strings, is operated in lake Baikal. We describe this first stationary underwater multistring array and present results from the first months of operation.

to be published in Proc. 3nd NESTOR Int. Workshop, Oct. 1993, Pylos, Greece

1 Introduction

The Baikal Neutrino Telescope [1,2] is being deployed in the southern part of the Siberian Lake Baikal, about 3.6 km from shore at a depth of 1.1 km. At this depths, the Baikal water has its minimal natural luminescence, the absorption length of light is about 20 m at λ=480-500 nm.

After several experiments with prototype configurations, temporary as well as stationary [3,4], during the past years, since April 13th, 1993 we are operating the stationary 3-string detector NT-36. This telescope is the first part of the Neutrino Telescope NT-200 [2] which will consist of a total of 192 optical modules.

As the first operating underwater array allowing for three-dimensional muon track reconstruction, NT-36 gives the possiblity to check the anticipated capabilities of this new type of detector, in particular with respect to pattern recognition and fake event rejection.

2 The Detector

The NT-36 is arranged at the same mechanical frame which will carry the NT-200 (Fig.1). The NT-200 system consists of 8 deep-underwater buoy stations arranged at the edges and the center of an equilateral heptagon. The strings are attached to a rigid frame consisting of 7 arms each 21.5 m in length. This umbrella-like frame is positioned 250 m above the bottom of the lake. The NT-36 modules (marked black in fig.1) are fixed to the central and two neighboring outer strings. Each string is equipped with half of the modules the full NT-200 strings would carry. To improve the performance of the smaller NT-36 detector, the arms were inclined, resulting in a decreased distance of 15.5 m between central and outer strings.

Two underwater electrical cables connect the detector site with the shore station. Deployment of all detector components is carried out during 7 weeks in late winter when the lake is covered by a thick layer of ice.

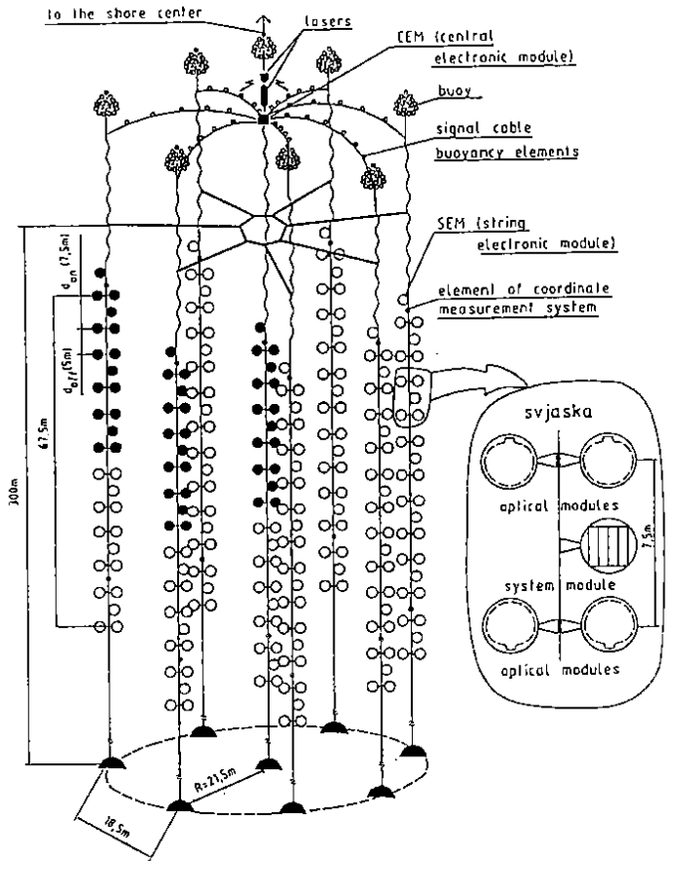

Fig.1: Schematical view of the planned NT-200 detector. The modules of NT-36, operating since April 1993, are in black.

The main component of the array is the underwater optical module (OM), equipped with a 37 cm diameter, highly sensitive phototube (QUASAR-370) with excellent resolution in time and amplitude [5]. The OMs are grouped in pairs along the strings, directed alternatively upward and downward. The distance between pairs looking face to face is 7.5 m, while pairs arranged back to back are 5 m apart. There are 6 pairs along each of the 3 strings of NT-36. The NT-36 configuration is sketched in fig.2.

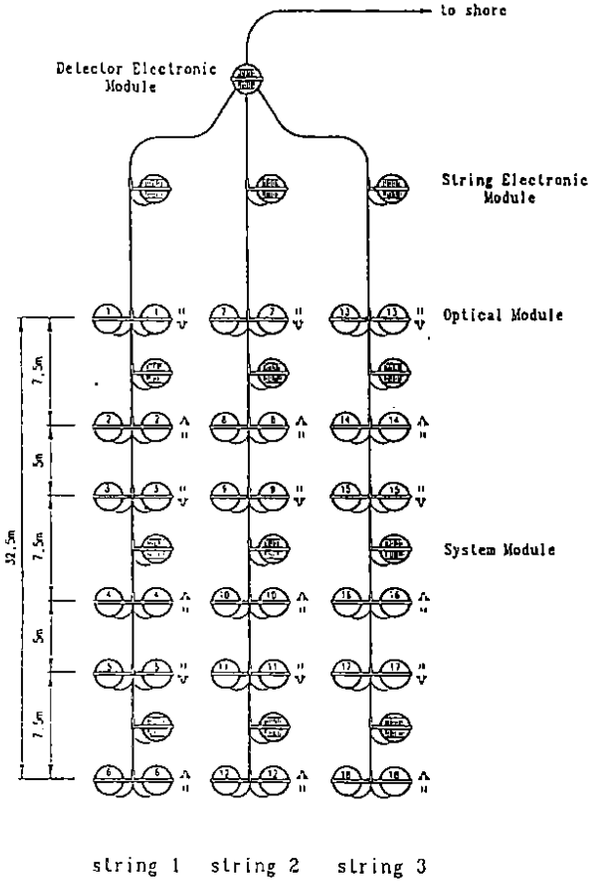

Fig.2: Schematical view of the NT-36 detector. The modules are numbered from 1-6 (string 1), 7-12 (string 2) and 13-16 (string 3). Even numbered modules are upward looking, odd numbered modules are oriented downward.

The two PMTs of a pair are connected in coincidence and define a *channel*, giving 18 channels for the NT-36 detector. The coincidence window has a width of 15 nsec. At a threshold of 0.3 photoelectrons (p.e.), the typical counting rate due to noise and bioluminescence is 50-100 kHz for a single QUASAR. By the coincidence, the rate is reduced

to 100-300 Hz per pair. This low counting rate is not only of significant advantage for underwater triggering and data transmission, but also leads to events nearly free from random hits (see below). The latter fact is essential for the difficult task of pattern recognition [6,7].

In case of a coincidence (*local trigger*), a data channel sends a request signal to the central electronic module. There, the *muon-trigger* is formed, by the requirement of $\geq m$ local triggers within a time window of 500 nsec. The threshold value m is set from shore to values between 2 and 5.

Once a muon trigger is formed, the amplitude and time digitizations, already initialized in the string electronic modules, are completed. The event record includes, in addition to the trigger generating channels, all local triggers within a time window of -1.0μsec to $+0.8\mu$sec with respect to the muon trigger signal.

Range and stepwidth of the amplitude system are 1000 p.e. and 1 p.e., respectively. An additional mode with 0.03 p.e. stepwidth and a range of 30 p.e. is used to calibrate the amplitude scale and to precisely determine the threshold using the single p.e. noise spectrum. The thresholds are set to values between 0.25 and 0.5 p.e.. In the normal mode, a calibration is performed using multi-p.e. signals from LEDs positioned in every OM. The time digitization system has a resolution of 1 nsec and a dynamic range of 2 μsec. Stability of the digitization is checked by calibration runs performed typically once every two days. To monitor their performance, the individual PMT rates as well as the local triggers for each channel are measured and transmitted to shore once per 30-60 sec.

The muon trigger system described above is tailored to events caused by the passage of a relativistic particle. A second system searchs for time patterns characteristic for slowly moving, bright particles like nuclearities or GUT magnetic monopoles catalyzing proton decays. Depending on the velocity of the object, such events could cause enhanced counting rates in individual channels during time intervals of 0.1 msec to 0.8 msec, separable from Poissonian noise [2].

The calibration of the relative time shifts between all channels of the array is performed with the help of a nitrogen laser of pulsewidth 300 psec positioned above the array. The light from this laser is guided by optical fibers of equal length separately to each OM pair. Complementary to this laser, at a distance of 67 m above the highest OM, there is a neodyme laser which emits light pulses directly into the water.

The spatial position of the components of the array is monitored by a hydroacoustical system. Signals from several ultrasonic emitters placed at radial distances of 600 m with respect to the telescope are registered

by receivers situated at the bottom and at the top of each of the three active strings. This system allows to determine of the positions with an accuracy better than the OM diameter (43 cm). A special "environmental" string positioned at a distance of 120 m from the telescope carries devices to measure the optical parameters of the water, temperature, pressure, sound velocity and water currents.

The data aquisition in the shore station is based on a robust and almost maintenance free configuration consisting of three PCs and a transputer network [8]. Fast data-preprocessing is done on the transputer system before data are stored on the main PC. This allows for error detection, event building and a completely asynchronous monitoring of the array performance. The latter employs visual checks of more than 200 histograms (stored on the transputer boards) on a graphical front-end PC.

3 First results

The array came into operation on April 13th, 1993 and is operated since this time. The main muon data taking runs were interrupted only due to calibration runs, operation of the environmental string, power failures and thunderstorms.

Generally, the components of the system show stable performance. Presently (December 1993), 23 of the 36 Optical Modules are still in operation. 9 OMs are dead and 4 are not accessible due to a failure of the corresponding system module (see fig.2). Altogether, 9 out of the originally 18 channels are still in operation. As far as one can judge, losses are due to failures of electronic components (e.g. HV supplies), not of the phototubes.

For standard muon runs, the trigger condition was set to 3/1 and 4/1, where trigger m/n stands for $\geq m$ hit channels on $\geq n$ strings. For 18 channels operating, the trigger rate was measured to be 10.06 ± 0.02 Hz for trigger 3/1 and 2.79 ± 0.01 Hz for trigger 6/3; this latter trigger was used to select the events for track reconstruction.

Table 1 gives a summary of trigger rates for the run periods with 18, 16 and 15 operating channels (April 13th-15th, April 17th-May 26th and May 27th-August 4th, respectively) for different off-line trigger conditions. To compare different run periods over the full time interval, we present for the 18 and 16 channels run periods also the trigger rates obtained by exclusion of those channels that ceased to operate in the 16 and 15 channel run periods, respectively. We note that the overall trigger

rate is falling with time, e.g. for the 15 channel configuration from 8.85 to 6.36 Hz over a period of 114 days. This is explained by effects like sedimentation, observed for upward looking modules already in earlier experiments [2]. Trigger rates based only on downward looking channels ($m/n(down)$), by contrast, are essentially constant (see table 1).

Array configuration	Trigger	Trigger Rates, Hz		
		Run145 15/04/93	Run 330 26/05/93	Run 680 04/08/93
18 channels	3/1	10.06 ± .020		
	4/1	7.43 ± .02		
	6/3	2.79 ± .01		
16 channels	3/1	9.11 ± .02	-	
	4/1	6.40 ± .02	5.31 ± .01	
	6/3	2.18 ± .01	1.491 ± .005	
	4/1(down)	0.405 ± .005	0.416 ± .003	
	6/3(down)	0.0474 ± .0015	0.0486 ± .0009	
15 channels	3/1	8.85 ± .02	-	6.36 ± .01
	4/1	6.10 ± .02	4.94 ± .01	3.95 ± .01
	6/3	1.96 ± .01	1.313 ± .005	0.896 ± .005
	4/1(down)	0.233 ± .003	0.237 ± .002	0.243 ± .003
	6/3(down)	0.0212 ± .0010	0.0214 ± .0006	0.0219 ± .0007

Table 1: Trigger rates for the Baikal Underwater Array NT-36 for the data taking periods with 18, 16 and 15 operating channels. Given are the main run for the first period, and the last runs for the 16 and 15 channel periods, respectively. Trigger condition "m/n" means $\geq m$ hit channels on $\geq n$ strings, "*down*" indicates consideration of downward looking channels only.

Fig.3a gives the muon trigger rates for individual channels (string 2) as a function of time (May 1st-May 31st) for trigger 4/1. Upward looking channels (8, 10 and 12) show almost steady decrease, whereas the downward channels (7, 9 and 11) are stable. Fig.3b gives the corresponding local trigger rates. All variations seen on this figure (apart from PMT-noise stabilisation after switch-on) are due to environmental effects - the local trigger rates strongly depend on the water luminosity. In spring and early summer, the local trigger rate was typically 100-200 Hz.

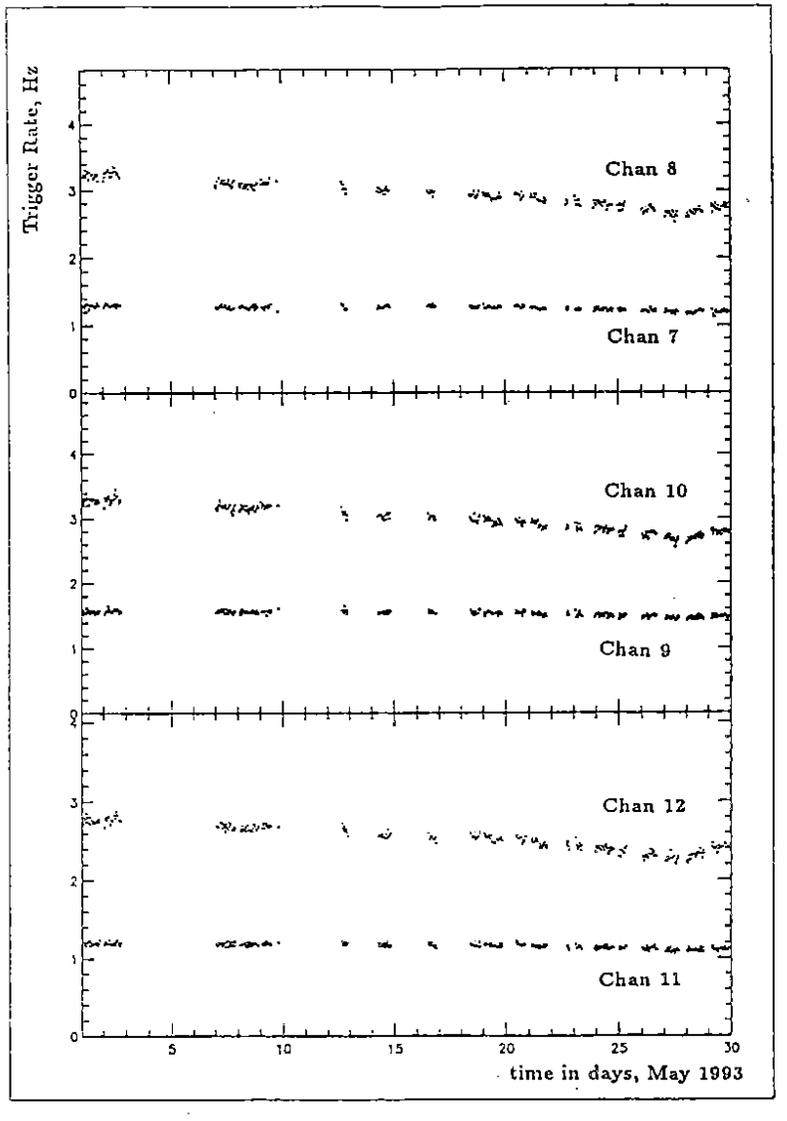

Fig.3a: Time dependence of the muon trigger rate for the channels on string 2 for May, 1993. The muon trigger condition was 4/1. Even channels are upward, odd channels are downward looking. Counting rates are averaged over 50 min, statistical errors are below 2%.

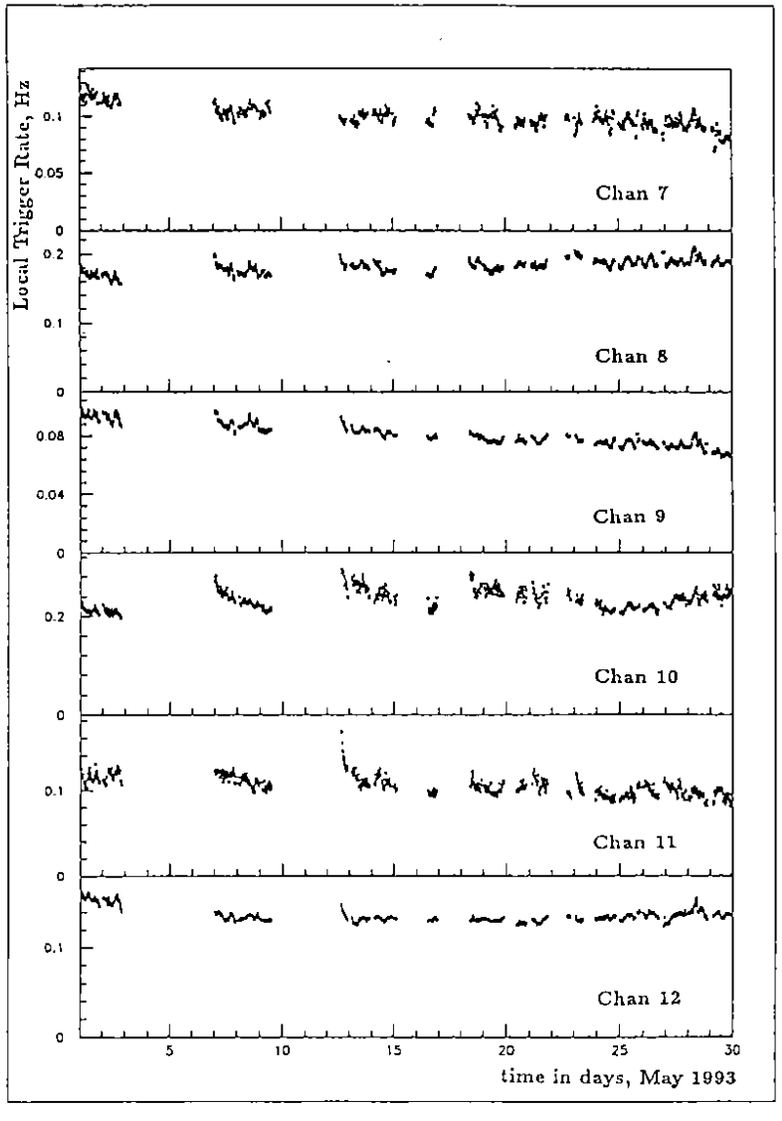

Fig.3b: Time dependence of the local trigger rates for the channels on string 2 for May, 1993, as measured independently of the muon trigger system. The counting rates are averaged over 30 min, statistical errors are below 0.3%.

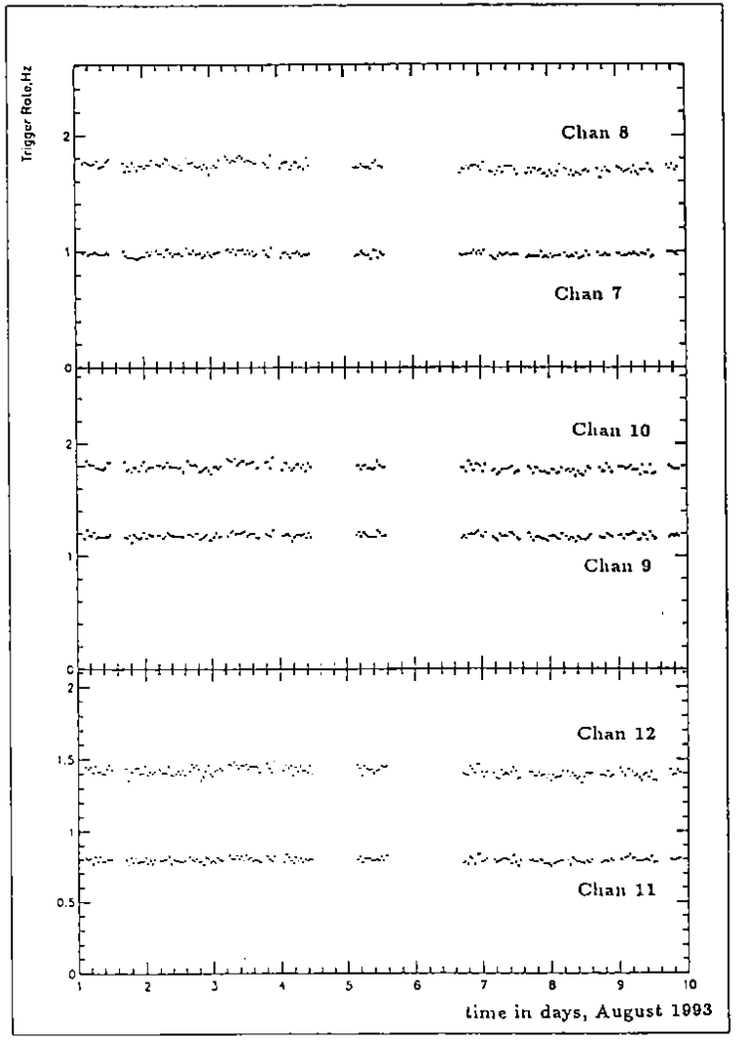

Fig.4a: Same as fig 3a but for the time period August, 1st-9th.

From August until mid September we observed an increase of the luminosity up to extremely high levels – sometimes the channel counting rates reached 2-2.5 kHz. At the end of September, the counting rates smoothly approached their original level.

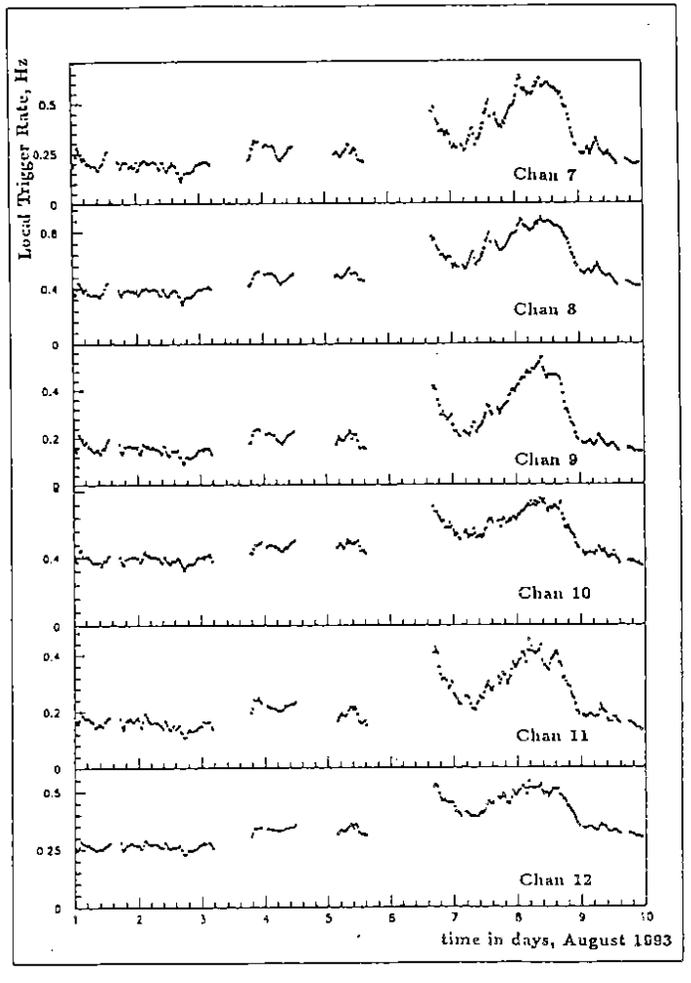

Fig.4b: Same as fig. 4b but for the time period August, 1st-9th.

The changes of the local trigger rate are not at all reflected in the muon trigger rate, since the muon trigger is essentially dominated by atmospheric muons, with negligible contribution by random (bioluminescence or noise) hits (see below). This is demonstrated in fig.4a and b, for a time interval of sharp changes of the local counting rates (August 1st-9th).

The muon trigger rate as a function of the number of hit channels N_{CH} is shown in fig.5 (18 operating channels). Also given are the predictions of our Monte Carlo (MC), normalized to the observed values at $N_{CH} = 3$. There, the absolute rates calculated by the MC coincide with the measured rate within the uncertainties of the integral muon flux at our depth ($\approx 10\%$). This was already shown with previous smaller prototype arrays [4]. The MC takes into account all known detector response effects and the stochastic nature of the muon energy loss. Reasonable agreement between the measured data and the MC calculation for $N_{CH} > 6$ is observed only if, in addition to single muons, also muon bundles are

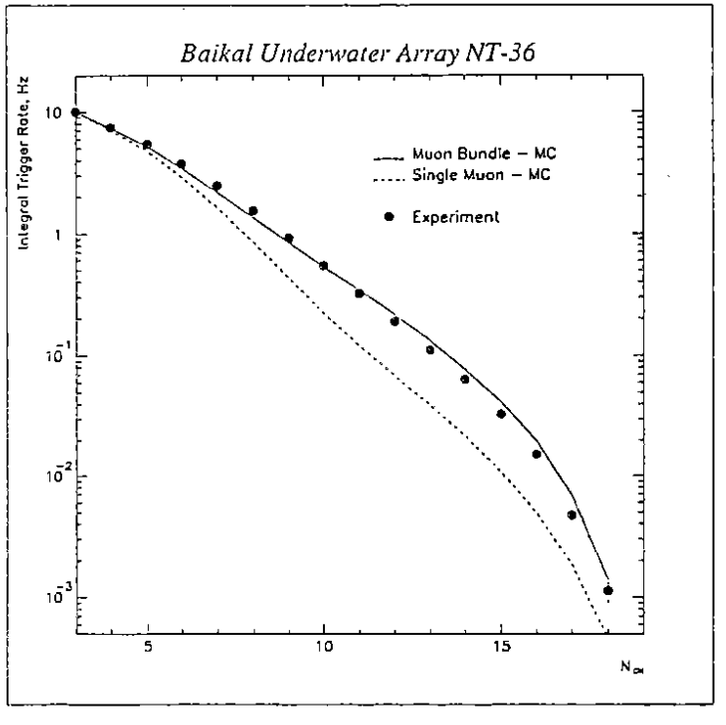

Fig.5: Integral trigger rate as function of the number of channels hit, N_{CH}. Points are experimental data (18 channel period, see table 1), the curves are MC calculations without (dotted line) and with (full line) inclusion of muon bundles.

taken into account (atmospheric shower simulation according to [9], normalized to the integral flux calculated from the sea level spectrum from [10]). Fig.6 gives the differential distribution of the number of hit channels, $P(N_{CH})$, for muon trigger 3/1 and the same data set as in fig.5. In fig.6a, the distribution for all channels is given, whereas in fig.6b and c the upward and downward channels are considered separately. We note that the basic features of all the data are reproduced by the MC; best quantitative agreement again is found for the muon bundle MC.

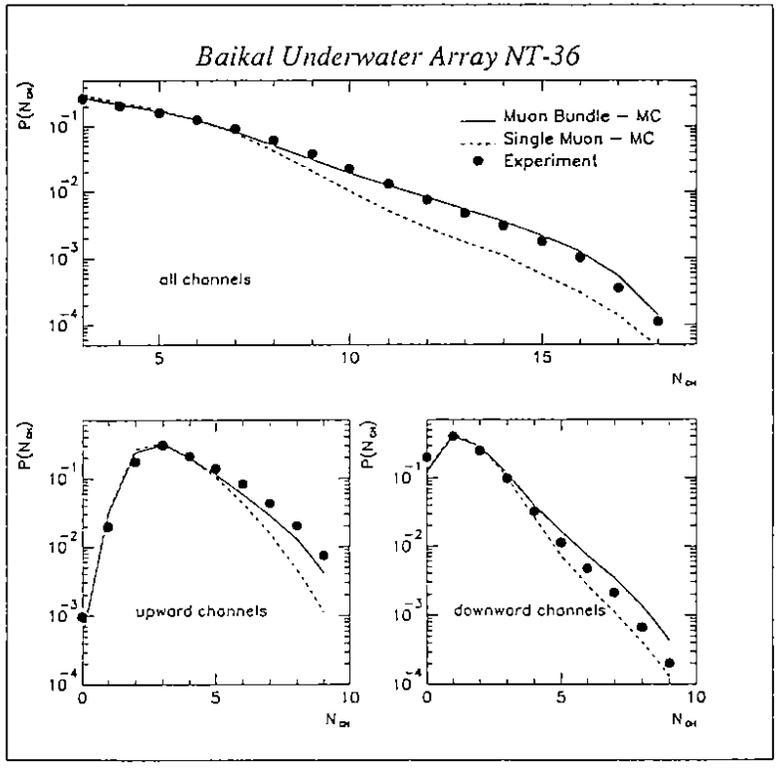

Fig.6: Differential distribution of the number of channels hit, N_{CH}, for the same run conditions as in fig.5. (a: All channels, b: Upward looking channels only, c: Downward looking channels only). Points are experimental data, the curves are MC calculations without (dotted line) and with (full line) inclusion of muon bundles.

Table 2 summarizes some characteristics of the NT-36 and the NT-200. For trigger 6/3, the effective area of NT-36 is calculated to be about 270 m^2 for 1 TeV muons. For 10 TeV muons it rises to 1000 m^2. The expected counting rate for atmospheric muons is $4.5 \cdot 10^7$ per year, for muons from neutrino interactions coming from the lower hemisphere it is 60 events per year (trigger 6/3).

For muon track reconstruction with Cherenkov telescopes, a precise relative timing of the different data channels is needed. Fig.7 illustrates the performance of the NT-36 laser time calibration system. The arrival times of the laser pulses, guided through fibres to the OMs, measure the relative time shift between all channels.

	NT-200	NT-36
number of PMT	192	36
number of strings	8	3
volume	$88.5 \cdot 10^3$ m^3	$3.04 \cdot 10^3$ m^3
effective area		
- for $E_\mu = 1$ TeV	2300 m^2	270 m^2
- for $E_\mu = 10$ TeV	4100 m^2	1000 m^2
median mismatch angle	1.3°	3.9°
# of downward μ	$3 \cdot 10^8$ y^{-1}	$4.5 \cdot 10^7$ y^{-1}
# of muons from upward atmospheric ν	490 y^{-1}	60 y^{-1}

Table 2: General characterestics of the Underwater Telescopes NT-200 and NT-36. Calculations are for trigger condition 6/3.

Fig.7 gives, for a laser run, the distribution of time differences $\Delta t_{i,j} = t_j - t_i$ between light arrival times t_i and t_j at channel i and j, respectively. It shows a narrow peak at zero for the laser pulses and a broad distribution for muonic events peaking at a value characteristic of the distance between the channels selected ($\Delta t \approx 83$ nsec for $\Delta x = 25$ m). The width of the laser peak ($FWHM \approx 2$ nsec) gives a conservative estimate of the time resolution of the whole system for large light amplitudes (A≈50 p.e.). For much smaller amplitudes, the PMT time jitter would be dominant. The laser is also used to measure the detection inefficiency of the individual channels, which is typically 0.08 and caused by dead time effects.

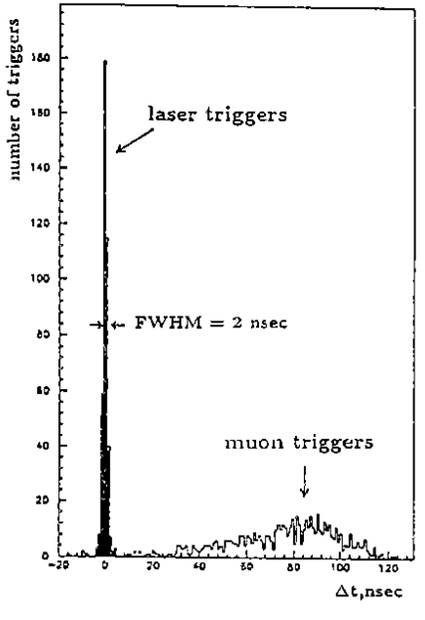

Fig.7: Distribution of light arrival time differences $\Delta t_{i,j} = t_j - t_i$ for channels 2 and 6 (string 1) for a typical laser run, with muon triggers recorded in parallel.

The distribution of light arrival time differences, $\Delta t_{i,j}$, for muon runs is given in fig.8 (channel 10 and 12 on string 2). The statistics corresponds to the full run period with at least 16 channels operating (table 1), i.e. $8.89 \cdot 10^6$ events for trigger 4/1 between April 14th and May 26th. We find a dominant peak around $\Delta t_{i,j} = 37.1$ nsec. It is essentially due to muons, as proved by the standard MC curve (dashed line). The almost

flat parts of the experimental distribution ranging up to ≈ -1000 nsec and $+1000$ nsec are originating from random non-muon hits in the muon trigger time window (500 nsec) as well as in the larger window considered once a trigger has been found (see above). For 100 Hz local counting rates, we expect a noise contribution of the order of 10^{-4} per channel per muon trigger. The quantitative behaviour of the noise contribution is well reproduced by the MC, once noise hits according to the true local counting rates are included. This MC prediction is shown by the full curve in fig.8.

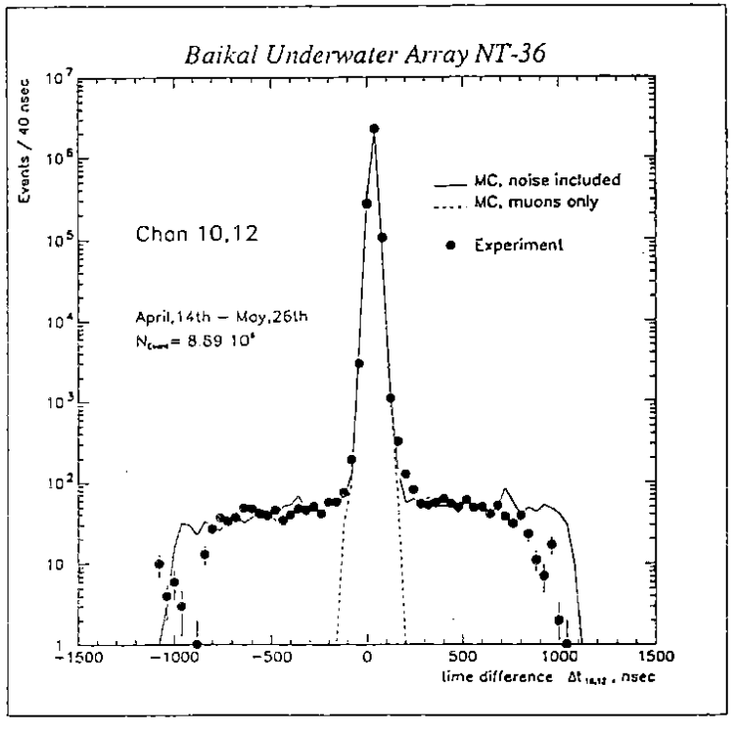

Fig.8: Distribution of light arrival time differences $\Delta t_{i,j} = t_j - t_i$ for channel 10 and 12 (string 2) for standard muon runs with trigger 4/1 recorded during the period with 16 operating channels (April 14th - May 26th). Points are experimental data, lines are results for the muon bundle MC without noise (dashed line)and with noise due to random hits (full line).

From this figure, we determine the noise rate experimentally to $1.01 \cdot 10^{-4}$ per channel per event for the full time window. For the restricted $\Delta t_{i,j}$ interval below the muon peak (−50...150nsec), the noise rate is reduced to $0.11 \cdot 10^{-4}$. For the full NT-36 and NT-200, the noise contribution from all channels for trigger 4/1 is about $2 \cdot 10^{-3}$ and $1 \cdot 10^{-2}$ noise channels per event, respectively.

In fig.9, we give the zoomed time difference distribution for the upward directed channels 8 and 12, as well as for channels 8 and 10. Monte Carlo and experiment (same run period as for fig.8) are found to coincide quite well.

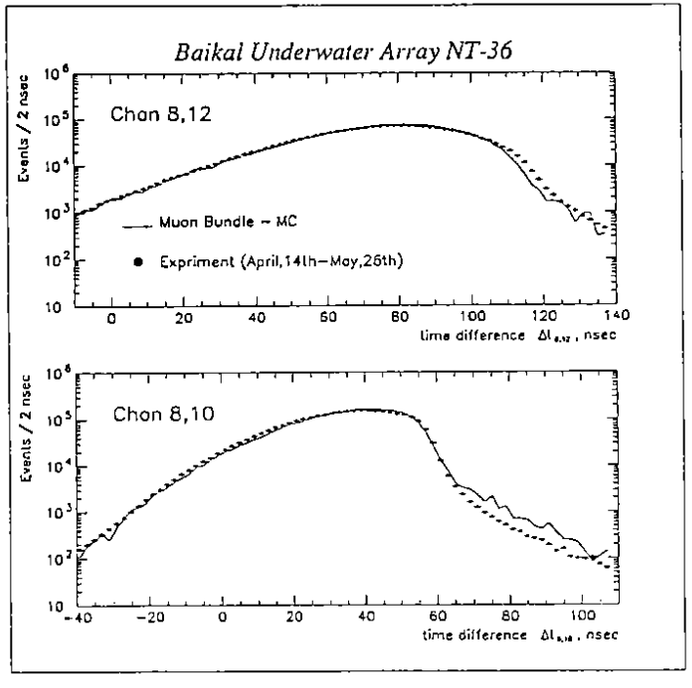

Fig.9: Distribution of light arrival time differences $\Delta t_{i,j} = t_j - t_i$ for channel 8 and 12 and for channels 10 and 12 (string 2) for standard muon runs with trigger 4/1, recorded during the period with 16 operating channels (April 14th - May 26th) for a zoomed time window with respect to fig. 8. Points are experimental data, the result for the muon bundle MC is given by the full line.

In parallel to the high energy neutrino and muon programme, we perform a search for slowly moving, bright particles like magnetic monopoles or strange quark nuclearities. These investigations are a continuation of studies that were performed with dedicated setups in lake Baikal between 1984 and 1988 [11]. From monopole induced proton decays [12] we would expect Cherenkov light signals generated by the decay products. For certain regions of the parameter space in β (monopole velocity) and σ_c (catalysis cross section), GUT monopoles would cause multiple hits in individual channels in time windows of 0.1-0.8 msec. To check our ability to detect rare signals above the Poissonian noise for a given sampling time window, we performed test runs in which the local triggers were sampled for time windows of 8 msec duration. Fig.10 gives the result of a test run of 2 hours for channels 14 and 18.

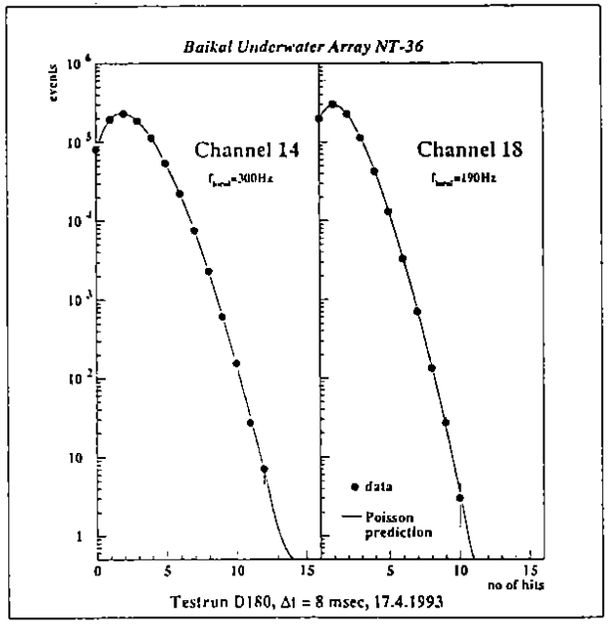

Fig.10: Distribution of the number of local triggers in a time window of 8 msec, as recorded with the monopole trigger system in a 2 hours testrun for channels 14 und 18 (string2). Experimental data are indicated by points, the curve gives the Poisson prediction, following from the measured local trigger rates.

We compare the number of local triggers detected within every 8 msec-time interval, N_{HIT}, with the calculated distribution. The calculation assumes pure Poisson statistics for the local trigger rate, according to the independently measured average local trigger rate (see e.g. fig.3b). Very good agreement with the Poisson assumption is deduced from fig.10, giving hope to reach the monopole limits envisaged in ref.[2] with the help of NT-200.

The light absorption coefficient κ, as measured in situ with the environmental string, is shown in fig.11 as a function of wave length λ.

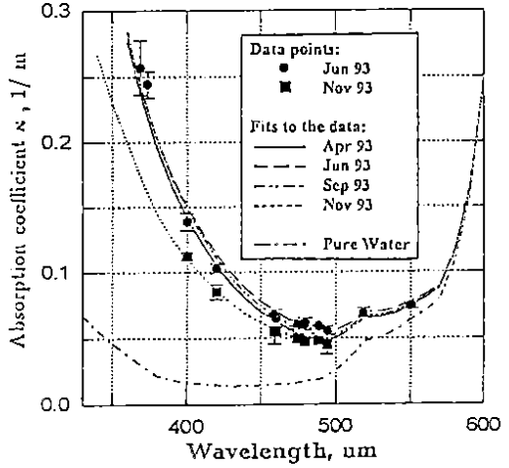

Fig.11: Absorption coefficient κ as function of wavelength λ, measured in situ from April - November 1993. Given are measured values for April and November (full symbols) and fits to the measurements (line).

The NT-36 array offers for the first time the possibility of a systematic study of the three dimensional track reconstruction capability of an underwater Cherenkov detector. This topic is discussed in detail in ref. [7]. As a final result we show in fig.12 the zenith angle distribution of reconstructed muon tracks and compare it wiht the MC results. Identical cuts were applied to the experimental and the MC data. Data are taken from the period with 16 channels operating and correspond to the statistics of one day. We investigated the full 16 channel run period and

did not find any significant time dependence of the reconstruction quality parameters or the rate of fake events.

Figs.8-9 and fig.12 demonstrate to what level we understand the response of our detector to muons. There are still a number of open questions, and, independently of the rather good agreement between data and MC, we are only at the beginning of a long process. We are continuing the data analysis and the development of the relevant tools. As an important preliminary result we quote the supression factor for downward going muons faking upward muons from ν-interactions, obtained with this comparably small array. Applying suitable track reconstruction methods and quality cuts, we achieved a factor of 10^4, in good agreement with our MC calculations, see [7]. Extrapolating this result to a 192-PMT array we conclude, confirming our earlier estimates [1,2,6], that NT-200 can operate as an efficient neutrino telescope with an angular acceptance of at least 70° around the opposite zenith.

During the 1994 winter expedition, we plan to haul up the array, repair failed components and deploy an upgraded array.

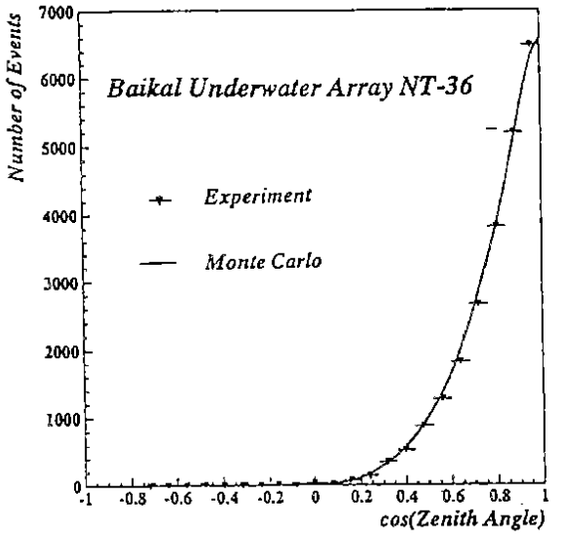

Fig.12: Zenit angle distribution for reconstructed muon tracks.

A part of this work is supported by the Volkswagen-Foundation

References

1. I.A.Belolaptikov et al., Nucl.Phys.B (Proc.Suppl.), 19 (1991) 17; I.A.Belolaptikov et al., Proc. 23rd ICRC, Calgary 1993, vol.4, 573
2. I.A.Sokalsky, Ch.Spiering (eds.), The Baikal Neutrino Telescope NT-200, BAIKAL 92-03
3. I.A.Belolaptikov et al., Proc. Third Int. Workshop on Neutrino Telescopes, Venice 1991, 365
4. I.A.Belolaptikov et al., Proc.XXVIth Int. Conf.High Energy Phys., Dallas 1992, vol.2, 1246
5. L.B.Bezrukov et al., Proc. 23rd ICRC, Calgary 1993, vol.4, 581; see contribution of B.K.Lubsandorzhiev to these proceedings: L.B.Bezrukov et al., Quasar-370 – The Optical Sensor of the Lake Baikal Neutrino Telescope, BAIKAL 93-17
6. I.A.Belolaptikov et al., Proc. 23rd ICRC, Calgary 1993, vol.4, 577
7. see contribution of Ch.Spiering to these proceedings: I.A.Belolaptikov et al., Track reconstruction and background rejection for the Baikal Neutrino Telescope, BAIKAL 93-16
8. H.Heukenkamp et al., Proc. 23rd ICRC, Calgary, 1993, vol.4, 585; H.Heukenkamp et al., to be publ. in Reihe "Informatik aktuell", Springer Verlag 1994, BAIKAL 93-08
9. S.N.Boziev et al., INR preprint P-0630, 1989
10. L.V.Volkova et al., Yad Fizika, 1979, vol.29(5), 1252
11. L.B.Bezrukov et al., Sov.J.Nucl.Phys., vol.52 (1990) 54
12. V.A.Rubakov, Rep.Progr.Phys., vol.51 (1988) 189